Influence of nanoporous structure on mechanical strength of aluminium and aluminium alloy adhesive structural joints

2006 J. Phys.: Condens. Matter 18 S2007

(http://iopscience.iop.org/0953-8984/18/33/S16)

INSTITUTE OF PHYSICS PUBLISHING JOURNAL OF PHYSICS: CONDENSED MATTER

J. Phys.: Condens. Matter **18** (2006) S2007–S2018 doi:10.1088/0953-8984/18/33/S16

Influence of nanoporous structure on mechanical strength of aluminium and aluminium alloy adhesive structural joints

C Spadaro, C Dispenza and C Sunseri

Dipartimento di Ingegneria Chimica dei Processi e dei Materiali, Università degli Studi di Palermo, Viale delle Scienze, 90128 Palermo, Italy

E-mail: c.spadaro@dicpm.unipa.it, dipenza@dicpm.unipa.it and sunseri@dicpm.unipa.it

Received 13 January 2006
Published 4 August 2006
Online at stacks.iop.org/JPhysCM/18/S2007

Abstract

The influence of surface treatments on the mechanical strength of adhesive joints was investigated. The attention was focused on AA2024 alloy because it is extensively used in both the automotive and aerospace industries. Adhesive joints fabricated with pure aluminium were also investigated in order to evidence possible differences in the surface features after identical treatments. Before joining with a commercial epoxy adhesive, metal substrates were subjected to different kinds of treatment and the surfaces were characterized by SEM analysis. The formation of a microporous surface in the AA2024 alloy, upon etching and anodizing, is discussed on the basis of the role of the intermetallic particles and their electrochemical behaviour with respect to the aluminium matrix. Moreover, nanostructured porous oxide layers on both type of substrate were also formed, as a consequence of the anodizing process. Differences in their morphologies were revealed as a function of both the applied voltage and the presence of alloying elements. On this basis, an explanation of the different values of fracture energy measured by means of T-peel tests carried out on the corresponding joints was attempted.

1. Introduction

Adhesive joints are a subject of high interest for possible applications in different fields, such as aerospace, transportation, packaging, biomedical and microelectronics [1, 2]. The general trend in engineering industries is to replace traditional fastening systems, such as riveting, nailing, and welding, with lighter and less corrosion sensitive bonding methods. Dissimilar engineering metals can be adhesively jointed with a reduced risk of galvanic corrosion; moreover, distortion resulting from the heat of welding is avoided and higher stiffness and energy absorption can be achieved [3, 4]. The widespread application of pure aluminium and its alloys in different industrial sectors, as either structural materials or coatings, has boosted

applied research activities by aerospace companies, defence agencies, research institutions and material suppliers in the field of adhesive bonding either aluminium to aluminium or aluminium to other metals, polymers, polymer composites, paper, wood, etc [1, 4–7]. Aluminium has high surface energy, good resistance in many aggressive environments, good formability, and high strength-to-weight ratio; therefore, it can greatly benefit from properties offered by adhesive bonding. The good resistance to corrosion attack of aluminium is due to its highly reactive surface forming an oxide layer instantaneously when it is exposed to the atmosphere. In order to improve adhesion to aluminium, the naturally formed oxide layer has to be removed, because it is nonuniform and does not form a stable base for structural bonding, and it has to be replaced with a new continuous and durable oxide form by means of either a single or a series of surface treatments [1, 3, 5, 8, 9]. Once the joint is assembled, an interface is formed between the metallic arms and the adhesive, that is characterized by a gradient in the properties from the pretreated adherend to the adhesive bulk. For structural adhesives, in particular, the interfacial phenomena play an important role in order to transfer the stresses between adherends and adhesive and poor durable bonds are often a consequence of poor interfacial properties [10, 11]. Therefore, the study of the surface treatments becomes a very noteworthy part in the structural design. The optimal surface preparation should be determined for the particular application and tested for both the initial strength and durability required.

Surface 'pre-treatments' of pure aluminium and its alloys can be grouped into three main types: mechanical, chemical, and electrochemical. Mechanical treatments, such as mechanical grinding or sandblasting, produce a highly micro-rough surface providing the possibility for mechanical interlocking [12]. Among the chemical treatments, the most extensively used is the Forest Product Laboratory Etch (FPL), based upon chromate solutions and widely applied in the aircraft and automotive industries, either as a stand-alone treatment or as pretreatment prior to anodizing [3, 5, 8]. The effect of this surface treatment is reported to be the formation of a rough fibrillated surface [5]. Recently, environmental restrictions have limited the use of chromate based solutions because the hexavalent form of chromium is a confirmed human carcinogen and forms many toxic compounds [13, 14]. For example, the EU directive 'end of vehicles', setting a new standard for scrapping, imposes a stepwise reduction in the use of hexavalent chromium in corrosion coating automotive [13]. Among electrochemical surface treatments, chromic acid anodizing was the one preferred by (European) aeroplane manufacturers for many years. In general, anodizing processes affect adhesion and durability of the structural joint depending on the electrochemically formed oxide film structure and thickness. This oxide is resistant to moist environments, although hydration of the surface has been observed [5].

Phosphoric acid anodizing (PAA) was also investigated and it is nowadays applied in aerospace and automotive industries, as also documented by both the Boeing BAC 5555 procedure [15] and the ASTM standards [16] that report the use of PAA after FPL and P2 etching [8], respectively.

Among the different electrochemical treatments for pure aluminium and its alloys, anodizing in phosphoric acid provides the most durable joints, also compared to the FPL etching process only [17]. It is generally expected that phosphoric acid anodizing produces a porous oxide layer on the metal surface with pores that are larger than the ones formed in chromic acid [7], thus creating sufficient roughness for mechanical interlocking. Nonetheless, it is well known that the pores of anodized aluminium may be as small as tens of nanometres in diameter and the question is whether any polymeric adhesive or primer could enter them, although electron microscopy and surface analysis have given evidence that polymeric adhesives can penetrate the microporous surface layer [17]. Moreover, the formed oxide layer protects the underlying metal from corrosive attack and favours chemical interaction (i.e. hydrogen bonding) with the adhesive [7, 9].

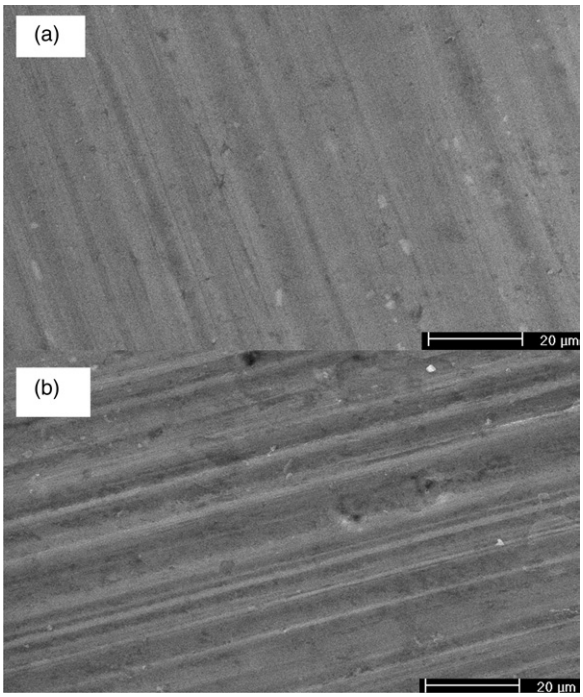

Figure 1. SEM micrographs of (a) pure aluminium and (b) AA2024 surfaces as received.

Table 1. Chemical composition of the investigated alloy (wt%).

Cu	Mg	Mn	Si	Fe	Al
4.19	2.18	0.62	0.5	0.5	Balance

In the present investigation, the adhesive strength of joints obtained using the same epoxy adhesive formulation with either AA2024 alloy or pure aluminium substrates, modified by applying an identical sequence of mechanical, chemical and electrochemical pre-treatments, is compared. The final goal is assessing how these two substrates are affected by the different treatments, in terms of both surface morphology and adhesive joints' mechanical performance, this last measured by means of T-peel tests. The large difference in intrinsic mechanical strength of the two adherends, as well as the difference in the substrates thickness, were taken into account in the algorithm used to calculate the fracture energy from the T-peel force, according to [18].

2. Experimental details

2.1. Materials

Pure aluminium (99.9%—0.1 mm thick) supplied by Becromal (Italy) and 0.64 mm thick AA2024-T3 aluminium alloy supplied by Cytec Engineered Materials were used as substrates. The chemical composition of the alloy is reported in table 1.

Pure aluminium samples were cut from a single rolled foil, while aluminium alloy samples were obtained from 230 mm × 300 mm sheets. The epoxy adhesive used was FM300K, supplied

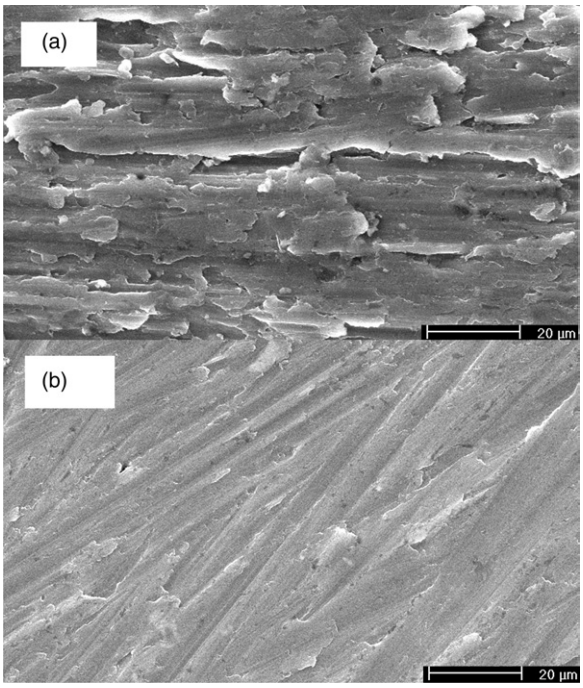

Figure 2. SEM micrographs of (a) pure aluminium and (b) AA2024 surfaces after mechanical grinding treatment.

by Cytec Engineered Materials (UK) in the form of a single rolled film, stored at −30 °C in air trapped boxes in the presence of silica gel until used.

2.2. Surface treatments

Coupons cut for subsequent morphological and mechanical characterization were subjected to the following surface treatments.

- *Degreasing.* The substrates were immersed in dichloromethane for 2 h and then thoroughly rinsed with deionized water.
- *Mechanical grinding.* 320 grit paper was used, then the samples were rinsed with deionized water.
- *Etching.* This treatment was carried out following the 'P2' procedure [8]. The coupons were kept under vigorous stirring for 10 min in a solution consisting of 370 g sulfuric acid (specific gravity 1.84), 150 g ferric sulphate and distilled water to 1 l. The temperature of the etching bath was controlled at 65 ± 1 °C. After etching, the coupons were thoroughly rinsed with deionized water.
- *Anodizing.* This treatment was conducted in 0.4 M phosphoric acid solution. Samples were anodically polarized by linear potential sweep at 0.2 V s^{-1} up to 10 or 120 V, then this potential was held for 20 min. A Glassman high tension (series ER) power source and a two electrode cell, having a Pt wire as the counter electrode, were used. The electrolyte temperature was 0 °C and it was controlled, within ±1 °C, by means of Lauda refrigerator (model RE 106). A vigorous stirring was maintained during the anodizing in order to guarantee a uniform distribution of temperature.

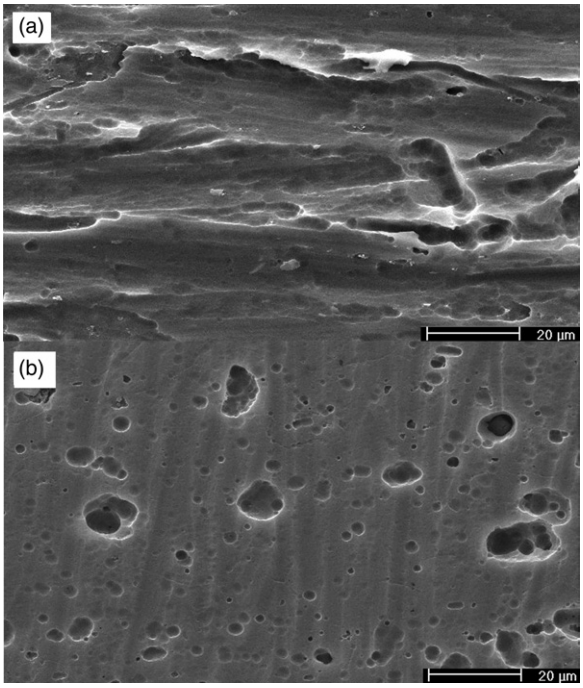

Figure 3. Low magnification SEM micrographs of degreased, mechanically ground and etched (a) pure aluminium and (b) AA2024 surfaces.

2.3. Surface characterization

The morphology of the substrates was characterized by means of scanning electron microscopy (SEM). The instrument used was a Philips ESEM XL30 scanning electron microscope. Prior to SEM examination, surfaces were sputter coated with gold. Surface analysis of the different substrates was carried out by energy dispersive spectroscopy (EDS) using a Philips PV 7760 probe.

2.4. Bonded joint preparation and testing

The surface treated substrates were assembled soon after the surface treatments and stored in sealed boxes in the presence of silica gel at −30 °C until curing. Adherents (100 mm × 20 mm) were overlapped by inserting, at one end, one 70 mm × 20 mm stripe of adhesive film. After the assembly, the joints were autoclave cured under a pressure of 2 bar. Thermal curing consisted of heating at 2 °C min^{-1} up to 175 °C, dwelling for 60 min, and cooling at 2 °C min^{-1} to room temperature. Once cured, the joints were stored in sealed boxes at −30 °C, in the presence of silica gel, until being mechanically tested.

Mechanical characterization was conducted by T-peel tests using an Instron (model 4443) universal testing machine with a load cell of 1 kN. The peel speed was 10 mm min^{-1}. Data from each run were elaborated following the Imperial College (London, UK) peel procedure [18].

3. Results and discussion

The effect of different surface treatments upon both pure aluminium and AA2024 alloy surfaces was investigated by means of morphological analysis and mechanical tests. SEM micrographs,

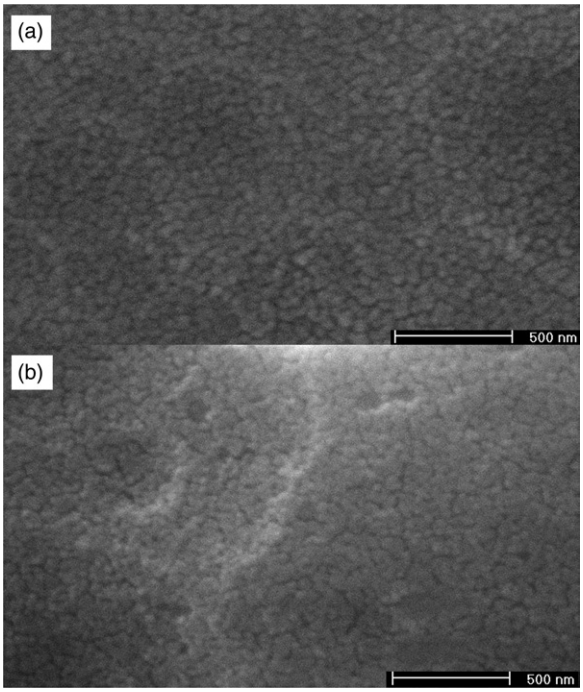

Figure 4. High magnification SEM micrographs of degreased, mechanically ground and etched (a) pure aluminium and (b) AA2024 surfaces.

reported in figure 1, show the pure aluminium (figure 1(a)) and the AA2024 (figure 1(b)) metal surfaces as received, while in figure 2 the corresponding morphologies after mechanical grinding are reported. As expected, the mechanical treatment with emery paper produced more pronounced ridges and grooves on the soft pure aluminium (figure 2(a)) than on the high strength AA2024 surface (figure 2(b)).

Figure 3 shows the modifications occurring after the P2 etching treatment. It can be observed that, whilst the morphology of pure aluminium presents elongated cavities and few pits, the aluminium alloy surface shows several pits, a few microns large, and rounded cavities up to 10 μm large. Conversely, at very high magnifications, the morphologies of pure aluminium and AA2024 surfaces are all similar, as shown in figures 4(a) and (b) respectively. The different morphologies observed at lower magnifications can be attributed to different rates of chemical attack of pure metal and alloy. The AA2024 alloy is less resistant to corrosion attack than pure aluminium [19], because of the microstructural heterogeneity at the metal surface due, predominantly, to the presence of intermetallic particles. Local galvanic cells form readily on the metal surface in aqueous environments because of the difference in electrochemical activity between these heterogeneous phases and between the particles and the matrix. The potential differences, due to the difference in electrochemical activity, provide the driving force leading to a severe and highly localized attack.

The electrochemical behaviour of AA2024 alloy has been widely investigated by several authors [20–26]. There is a general agreement about the cathodic nature of the Al–Cu–Mn–Fe–Si, while the electrochemical behaviour of the Al–Cu–Mg particles is not fully clarified. Some authors claim a transformation of these particles, identified as Al_2CuMg, from anodic to cathodic sites during immersion in the electrolyte, due to a dealloying process leading to a

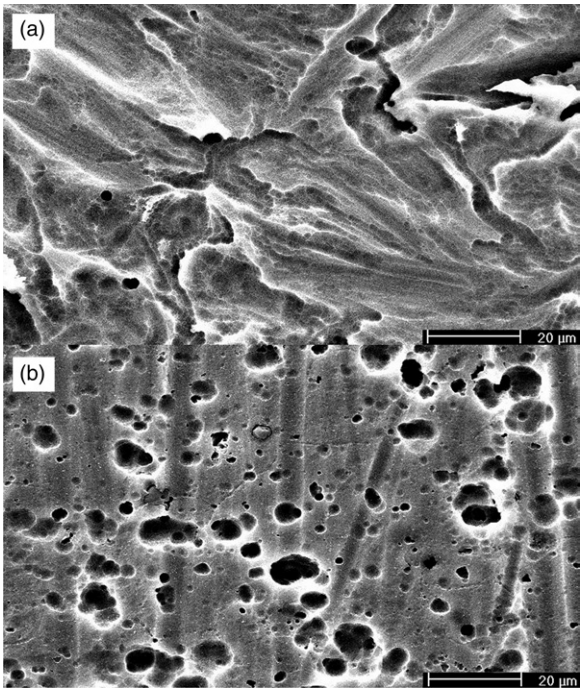

Figure 5. Low magnification SEM micrographs of degreased, mechanically ground, etched, and 120 V anodized (a) pure aluminium and (b) AA2024 surfaces.

preferential dissolution of Mg and Al and, thus, to a local enrichment of Cu [27, 28]. Therefore, a significant attack on the surface where the Al–Cu–Mg particles were located can occur, due to their selective dissolution, leaving pits where particles resided. Furthermore, a pitting attack is also expected where noble particles with respect to the matrix are located and, in this case, pits are formed at their periphery. The cavities observed for AA2024 alloy can be due to both coalescence of pits and undermining of noble particles.

After mechanical and chemical treatment of the surfaces, samples were anodized in phosphoric acid solution. Following a procedure reported in the literature [29, 30], the voltage was initially swept up to the final desired value and, then, it was held for 20 min in order to form the oxide layer. After reaching the final value of potential, the current density, for both pure aluminium and AA2024 alloy, after an initial rapid decay, slowly decreased, reaching a steady-state value. This behaviour is due to the formation of a passive layer covering the underlying metal. The observed low value of steady-state current is indicative of the high electrical resistance of the film formed during the anodization, which can behave as either insulator or semiconductor. Figure 5 shows the typical morphology of both pure aluminium (figure 5(a)) and AA2024 (figure 5(b)), respectively, after anodizing at the highest voltage (120 V).

As far as pure aluminium is concerned, it can be noticed that there is not a significant difference in the morphology with respect to the corresponding etched substrate, whereas a high population of macro-pores is formed in AA2024 surface during anodizing. This last effect is probably due to the enhancement of the corrosion attack during the anodizing process. This hypothesis is confirmed by the results of EDS analysis, presented in table 2, where molar ratios of aluminium to copper and magnesium are reported. The ratio Al/Cu is practically constant,

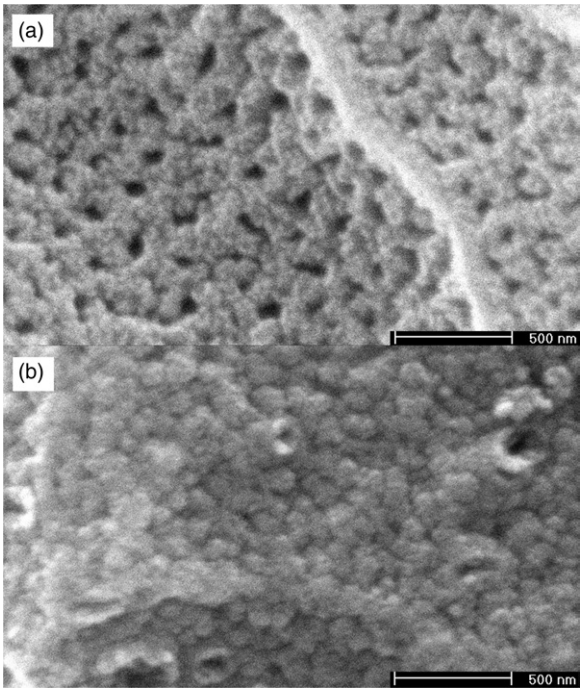

Figure 6. High magnification SEM micrographs of degreased, mechanically ground, etched, and 120 V anodized (a) pure aluminium and (b) AA2024 surfaces.

Table 2. Molar ratios between aluminium and other alloying components after etching and anodizing.

Before surface treatments		After surface treatments	
Al/Cu	Al/Mg	Al/Cu	Al/Mg
22.20	42.66	22.28	236.2

indicating that there was no loss of Cu, while the ratio Al/Mg was significantly increased upon etching and anodizing, thus confirming the preferential dissolution of Al and Mg from Al_2CuMg particles.

In this context, we must consider that EDS analysis was conducted on a large surface area; therefore, aluminium from both matrix and intermetallic particles was revealed. Since Al_2CuMg particles cover 2.7% of the total alloy surface [28], the EDS peak of Al was essentially due to the matrix, while the Mg peak was due to the remnant particles. For this reason, a large increase in the Al/Mg ratio, despite the dissolution of aluminium from the intermetallic particles, was observed. At higher magnifications, the surfaces show the morphologies presented in figure 6: both surfaces present nanoroughness, but while pure aluminium (figure 6(a)) is covered by a nanoporous structured layer with 65 nm average diameter pores, AA2024 (figure 6(b)) shows a globular structure with pores much smaller in size than those for pure aluminium. The formation of a porous structure on aluminium by electrochemical oxidation of the metal is well known and it is due to localized dissolution of oxide assisted by the electric field at the electrode/electrolyte interface [31–34].

Taking into account that the same anodizing voltage, which is the fundamental parameter controlling the porous structure [19, 31–35], was applied to both pure aluminium and AA2024,

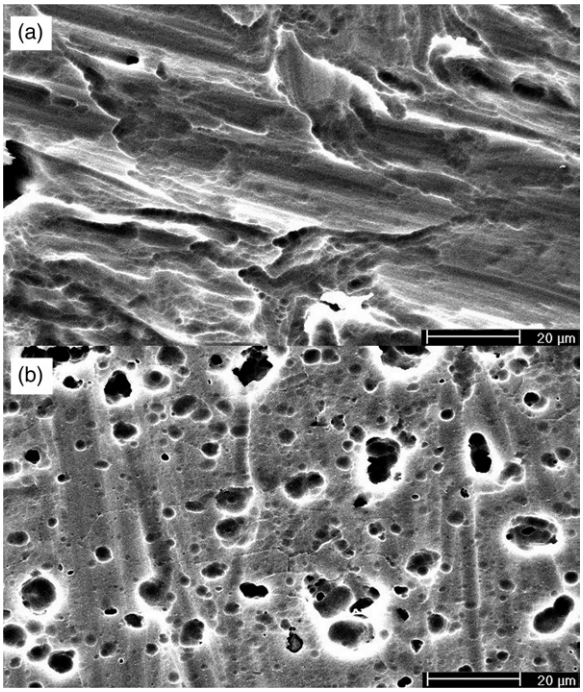

Figure 7. Low magnification SEM micrographs of degreased, mechanically ground, etched, and 10 V anodized (a) pure aluminium and (b) AA2024 surfaces.

quite interestingly, figure 6(b) shows that the addition of some alloying element to pure aluminium modifies the grown porous structure.

At the applied voltage of 10 V, which is the typical phosphoric acid anodizing condition reported in both the literature and the standard procedures [8, 16, 36–39], the morphologies of pure aluminium and AA2024, as observed at lower magnification (see figures 7(a) and (b)) resemble those shown for the voltage of 120 V; in contrast, at the higher magnification shown in figures 8(a) and (b), it can be noticed that the oxide layer grown onto pure aluminium maintains a nanoporous structure, but with a much smaller average pore diameter, whilst the AA2024 surface appears much smoother than at 120 V. The pore size increase with the anodizing potential is in good agreement with the literature data on electrochemically grown porous aluminium oxide [35] (compare figures 6(a) and 8(a)).

In order to characterize the mechanical behaviour of the joints produced with either etched or etched and anodized substrates at different voltages, T-peel tests were carried out and fracture energies were calculated from the measurement of peel forces, according to the analytical relations reported in [18]. The results of mechanical tests are shown in figure 9. Fracture energies of joints made with only degreased and mechanically ground adherends are also reported for comparison.

It can be observed that all treatments carried out after degreasing and mechanical grinding increase the adhesive fracture energy of both pure aluminium and AA2024 joints. The best results, in both cases, were the ones obtained with etched and 120 V anodized adherends. It is noteworthy to point out that the etching treatment of a mechanically ground surface has the effect of transforming the nature of the fracture from mainly adhesive (i.e. running at the adhesive–adherend interface) to mainly cohesive (i.e. partially running across the adhesive

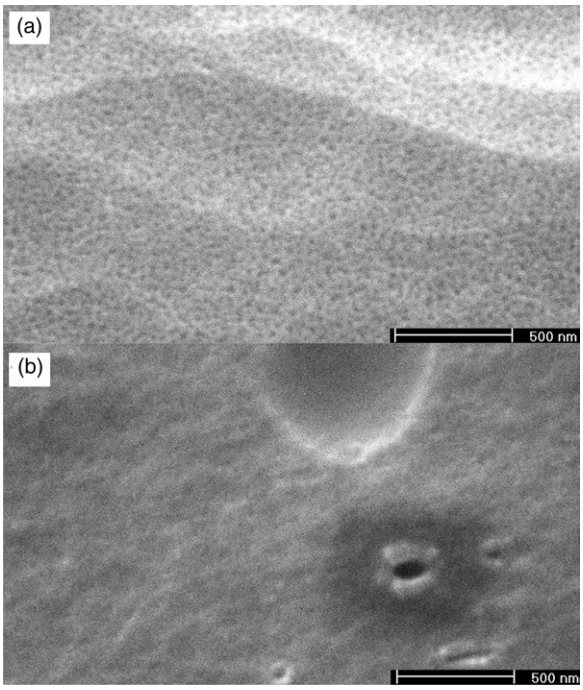

Figure 8. High magnification SEM micrographs of degreased, mechanically ground, etched, and 10 V anodized (a) pure aluminium and (b) AA2024 surfaces.

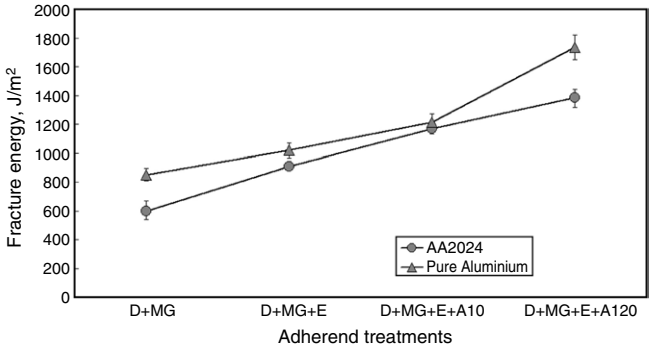

Figure 9. Influence of adherend treatment on fracture energy for pure aluminium and AA2024 joints. D = degreased, MG = mechanically ground, E = etched, A10 = anodized at 10 V, A120 = anodized at 120 V.

bulk) and improving the consistency of the mechanical testing results, especially for AA2024. This effect is probably due to a more effective adhesive–adherend mechanical interlocking, promoted by the etching treatment leading to the formation of pits and cavities on both pure aluminium and AA2024 alloy, as already shown in figure 3. Furthermore, the adhesive fracture energy of pure aluminium joints is always higher than for AA2024 joints and again, in an attempt to understand the particular features of the mechanical behaviour of the different joints, the SEM morphologies already discussed have to be taken into account. As far as pure aluminium is concerned, the main modification in the substrate morphology is obtained when

anodizing is applied after etching. As already shown in figures 6(a) and 8(a), the structure of the electrochemically grown oxide layer is nanoporous, thus significantly increasing the surface specific area and improving the extent of interaction with the adhesive, in the assumption though that the adhesive can enter into the pores. Of course, this is the more likely to occur the larger are the pores, and, not surprisingly, the highest value of fracture energy was measured at the highest anodizing voltage. Furthermore, it cannot be excluded that, in these conditions, a more hydrated oxide layer is also formed [40] which should induce both improved wettability and chemical bonding with the epoxy adhesive (chemisorption). Further investigations are in progress in order to better elucidate this issue.

It is noteworthy that the very low pore size on anodized AA2024 determined lower values of fracture energy for AA2024 joints, with respect to the pure aluminium analogues, indicating how appropriate sized nanoporous structures can play a fundamental role in improving the joint adhesion. In this context, it is interesting to point out that also the anodizing voltage is an important parameter in determining the mechanical resistance of the adhesive joints, since the interaction at the interface between adhesive and adherends increases with the applied voltage.

4. Conclusions

The role of some kind of surface treatments upon both pure aluminium and AA2024 alloy on the mechanical strength of adhesive joints was investigated. After degreasing and mechanical grinding, specimens were etched and anodized in a phosphoric acid bath. The differences in the surface morphologies of the two substrates after each treatment can help to explain the corresponding differences in the adhesive joints' mechanical performance. Generally, each treatment produces an increase of fracture energy for both types of bonded substrate. The effect of the chemical etch is more pronounced for the AA2024 substrates, which showed a lower resistance to the corrosion attack, due to the presence of intermetallic particles in the alloy. The pits and cavities formed, permeated by the adhesive, can be responsible for mechanical keying, thus improving adhesion. The subsequent anodizing step enhanced the corrosion attack on AA2024 substrate only, as revealed by the increase of macro-porosity, and at the same time promoted the growth of a nanostructured oxide porous layer on both substrates. Quite interestingly, the pore size is affected by both the applied voltage and the presence of the alloying elements. The highest pore size observed was obtained for the pure aluminium substrates anodized at 120 V, which also displayed the highest increase in the fracture energy of the corresponding joints. Of course, chemical modification of the substrates upon anodizing cannot be excluded, thus suggesting chemisorption as a possible cooperating mechanism in the adhesion improvement.

Acknowledgments

The authors would like to acknowledge Professor R Moore of Imperial College for valuable help in T-peel testing and data elaboration, and Dr P T McGrail and Dr S Ward of Cytec Engineered Materials for the supplied materials and helpful discussion.

References

[1] Petrie E M 2000 *Handbook of Adhesives and Sealants* (New York: McGraw Hill) p 17, 596, 232
[2] Kinloch A J 1997 *Proc. Inst. Mech. Eng.* G **211** 307
[3] Lunder O, Olsen B and Nisancioglu K 2002 *Int. J. Adhes. Adhesives* **22** 143
[4] Higgins A 2000 *Int. J. Adhes. Adhesives* **20** 367

[5] Critchlow G W and Brewis D M 1996 *Int. J. Adhes. Adhesives* **16** 255
[6] Starke E A Jr and Staley J T 1996 *Prog. Aerospace Sci.* **32** 131
[7] Armstrong K B 1997 *Int. J. Adhes. Adhesives* **17** 89
[8] Digby R P and Packam D E 1995 *Int. J. Adhes. Adhesives* **15** 61
[9] van de Brand J, Van Gils S, Beentjes P C J, Terryn H, Sivel V and de Wit J H W 2004 *Prog. Org. Coat.* **51** 339
[10] LeFebvre D R, Ahn B K, Dillard D A and Dillard J G 2002 *Int. J. Fract.* **114** 191
[11] Kinloch A J, Little M S G and Watts J F 2000 *Acta Mater.* **48** 4543
[12] Harris A F and Beever A 1999 *Int. J. Adhes. Adhesives* **19** 445
[13] Directive 2000/53/EC of the European Parliament and of the council of 18 September 2000 on end-life vehicles *Off. J. Eur. Communities* L269/34
[14] Fahrenholtz W G, O'Keefe M J, Zhou H and Grant J T 2002 *Surf. Coat. Technol.* **155** 208
[15] BAC 5555 revision A1975 Boeing process specification phosphoric acid anodizing of aluminium for structural bonding
[16] ASTM D3933-98 (reapproved 2004) standard guide for preparation of aluminium surfaces for structural adhesives bonding (phosphoric acid anodizing)
[17] Packam D E 1998 The mechanical theory of adhesion—a seventy year perspective and its current status *1st Int. Congr. on Adhesion Science and Technology (Invited Papers) (Utrecht 1998)* ed W J van Ooj and H R Anderson Jr (Leiden: VSP Publishers) pp 81–108
[18] Moore D R and Williams J G 2001 *Fracture Mechanics Testing Methods for Polymers, Adhesives and Composites, ESIS Publication 28* ed D R Moore, A Pavan and J G Williams (Oxford: Elsevier)
[19] Wernick S, Pinner R and Sheasby P G 1987 *The Surface Treatment and Finishing of Aluminium and its Alloys* 5th edn, vol 1 (Middlesex: Finishing Publications Ltd) p 4
[20] Buchheit R G 1995 *J. Electrochem. Soc.* **142** 3994
[21] Blanc C, Lavelle B and Mankowski G 1997 *Corros. Sci.* **39** 495
[22] Schmutz P and Frankel G S 1998 *J. Electrochem. Soc.* **145** 2295
[23] Liao C M and Wei R P 1999 *Electrochim. Acta* **45** 881
[24] Campestrini P, van Westing E P M, van Rooijen H W and de Wit J H W 2000 *Corros. Sci.* **42** 1853
[25] Zhang W and Frankel G S 2002 *J. Electrochem. Soc.* **149** B510
[26] Zhang W and Frankel G S 2003 *Electrochim. Acta* **48** 1193
[27] Chen G S, Gao M and Wei R P 1996 *Corrosion* **52** 8
[28] Buchheit R G, Grant R P, Hlava P F, Mackenzie B and Zender G L 1997 *J. Electrochem. Soc.* **144** 2621
[29] Bocchetta P, Sunseri C, Bottino A, Capannelli G, Chiavarrotti G, Piazza S and Di Quarto F 2002 *J. Appl. Electrochem.* **32** 977
[30] Bocchetta P, Sunseri C, Chiavarrotti G and Di Quarto F 2003 *Electrochim. Acta* **48** 3175
[31] Diggle J W, Downie T C and Goulding C W 1969 *Chem. Rev.* **69** 370
[32] Siejka J and Ortega C 1977 *J. Electrochem. Soc.* **124** 883
[33] Parkhutik V P and Shershulsky V J 1992 *J. Phys. D: Appl. Phys.* **25** 1258
[34] Sunseri C, Spadaro C, Piazza S, Volpe M and Di Quarto F 2006 *J. Solid State Electrochem.* **10** 416
[35] O'Sullivan J P and Wood G C 1970 *Proc. R. Soc.* A **317** 511
[36] Bjørgum A, Lapique F, Walmsley J and Redford K 2003 *Int. J. Adhes. Adhesives* **23** 401
[37] Johnsen B B, Lapique F, Bjørgum A, Walmsley J, Tanem B S and Luksepp T 2004 *Int. J. Adhes. Adhesives* **24** 183
[38] Johnsen B B, Lapique F and Bjørgum A 2004 *Int. J. Adhes. Adhesives* **24** 153
[39] Comyn J, Day J and Shaw S J 1997 *Int. J. Adhes. Adhesives* **17** 213
[40] Despic A and Parkhutick V 1989 *Modern Aspects of Electrochemistry* No. 20 ed J O' Bockris, R E White and B E Conway (New York: Plenum) p 412